NANO · MICRO small
www.small-journal.com

Oxidase-Like Fe-N-C Single-Atom Nanozymes for the Detection of Acetylcholinesterase Activity

*Yu Wu, Lei Jiao, Xin Luo, Weiqing Xu, Xiaoqian Wei, Hengjia Wang, Hongye Yan, Wenling Gu, Bo Z. Xu, Dan Du, Yuehe Lin, and Chengzhou Zhu**

Single-atom catalysts (SACs) have attracted extensive attention in the catalysis field because of their remarkable catalytic activity, gratifying stability, excellent selectivity, and 100% atom utilization. With atomically dispersed metal active sites, Fe-N-C SACs can mimic oxidase by activating O_2 into reactive oxygen species, O_2^{-}• radicals. Taking advantages of this property, single-atom nanozymes (SAzymes) can become a great impetus to develop novel biosensors. Herein, the performance of Fe-N-C SACs as oxidase-like nanozymes is explored. Besides, the Fe-N-C SAzymes are applied in biosensor areas to evaluate the activity of acetylcholinesterase based on the inhibition toward nanozyme activity by thiols. Moreover, this SAzymes-based biosensor is further used for monitoring the amounts of organophosphorus compounds.

1. Introduction

Nanozymes, a series of bioinspired nanomaterials with enzyme-like catalytic ability, have aroused tremendous interest in fields of biosensing, biomedical systems, and environmental governance ever since the report of peroxidase-mimicking Fe_3O_4 nanoparticles in 2007.[1] For one thing, nanozymes owe advantages like high catalytic activity, low cost, and easy to be prepared in large quantities. For another, nanozymes overcome part limits of natural enzymes such as low tolerance toward pH, temperature, and the organic solvent, activity damage in long period usage and difficulties in purification. Until the date, many nanomaterials (e.g., carbon, noble metal materials, and metal oxides),[2] have been covered to catalyze some reactions which used to be done by the natural enzymes. Though the crucial progress being achieved, tremendous challenges like complex catalytic mechanism, poor catalytic selectivity, and limited catalytic activity hinder the continuous development of nanozymes due to the great complexity in terms of atomic composition and structure of nanomaterials.

Metal-based nanomaterials are the main class of heterogeneous catalysts. One prominent character of them is that the catalytic performances can be improved by decreasing the size of metal nanoparticles. Downsizing catalyst nanoparticles to single-atom scale can lead to the maximized atom utilization and the enhanced catalytic activity.[3] Since the pioneering work of single-atom catalysts (SACs) was reported by Zhang and co-workers,[1e,4] various SACs emerged, which arouse extraordinary amounts of interest in different fields.[5] Among these SACs, M-N-C nanostructures have gained plentiful eyes due to the diverse synthetic approaches and superior catalytic activity.[6] Specifically, coupling with rational designs and advanced characterizations, M-N-C SACs show distinctive electrocatalytic activity toward small molecules. It is noted that the synergistic effects arising from the strong metal-support interactions play a critical role in boosting their catalytic performances and realizing the in-depth understanding of the structure-activity relationship at the atomic scale. M-N-C SACs are promising candidates to serve as novel nanozyme models due to the fact that active sites present similar structures with MN_x sites of natural enzymes.[7] Recently, M-N-C-based single-atom nanozymes (SAzymes) with multiple enzyme-like activities were reported.[8] For example, Shi and co-workers applied Fe-N-C SAzymes in tumor therapy.[9] In addition, Zn-N-C SAzymes with peroxidase-like activity were investigated and applied for wound antibacterial.[10] Single CoN_4 sites exhibit eminent Fenton-like activity for the remediation of organic pollutants.[11] Inspired from these pioneering works and combined with reported applications of nanozymes in the sensing area,[12] SAzymes are greatly expected for construction of the novel biosensors.

Herein, we demonstrated the splendid oxidase-like Fe-N-C SAzymes. With the ability to catalyze the transformation of O_2

Y. Wu, L. Jiao, X. Luo, W. Xu, X. Wei, H. Wang, H. Yan, Prof. W. Gu, Prof. C. Zhu
Key Laboratory of Pesticides and Chemical Biology of Ministry of Education
International Joint Research Center for Intelligent Biosensing Technology and Health
College of Chemistry
Central China Normal University
Wuhan 430079, P. R. China
E-mail: czzhu@mail.ccnu.edu.cn
Dr. B. Z. Xu
Department of Materials Science and Engineering
University of California
Berkeley, CA 94720, USA
Prof. D. Du, Prof. Y. Lin
School of Mechanical and Materials Engineering
Washington State University
Pullman, WA 99164, USA
The ORCID identification number(s) for the author(s) of this article can be found under https://doi.org/10.1002/smll.201903108.

DOI: 10.1002/smll.201903108

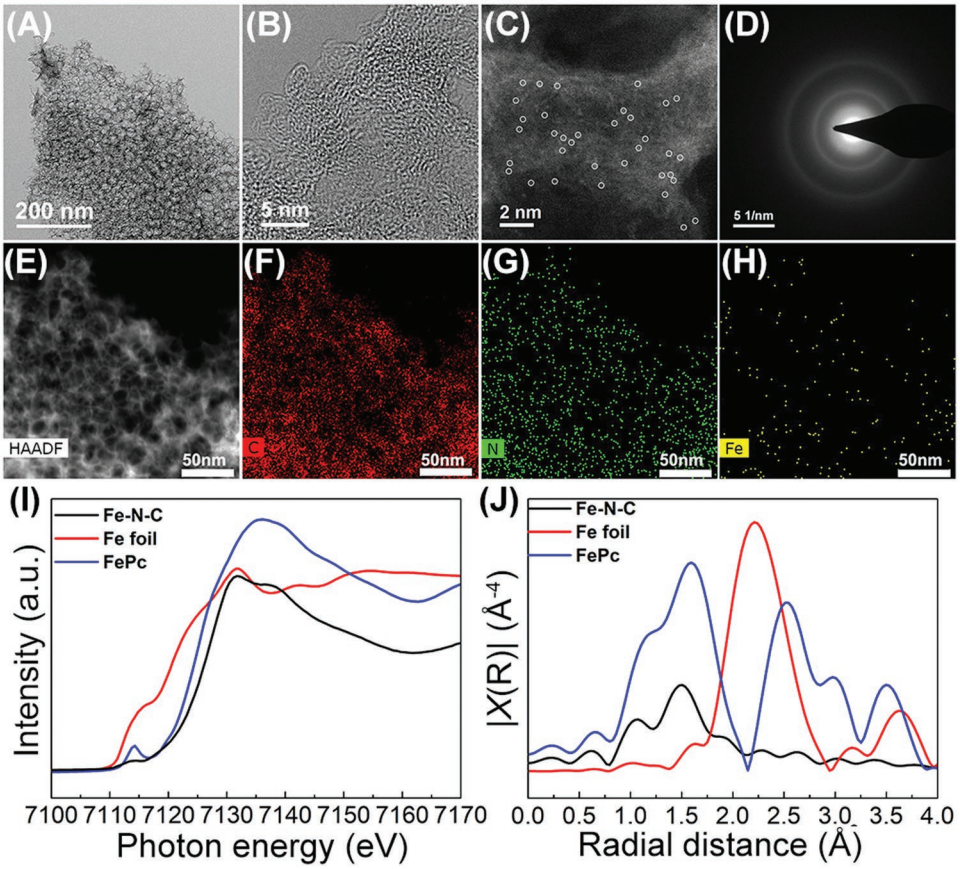

Figure 1. A) TEM image, B) HR-TEM image, C) HAADF-STEM image (Z-contrast), and D) SAED pattern of Fe-N-C SAzymes. E) HAADF-STEM image and F–H) the corresponding EDS elemental distribution of the C, N, and Fe atoms in the Fe-N-C SAzymes. I) Fe K-edge XANES spectra and J) Fourier-transform EXAFS spectra of Fe-N-C SAzymes, reference Fe foil, and FePc.

into reactive oxygen species, superoxide radicals (O_2^{-}•), Fe-N-C SAzymes can trigger some allochroic reactions. Interestingly, it was found that mercapto molecules can bind to Fe-N-C SAzymes and inhibit the nanozyme activity. On this basis, we successfully fabricated a Fe-N-C SAzymes-based biosensor to evaluate the activity of acetylcholinesterase (AChE). Also, the AChE-Fe-N-C SAzymes system was further used for monitoring the amounts of organophosphorus compounds (OP). This work not only provides novel oxidase-like SAzymes, but also paves an avenue for evaluating enzyme activity and other related biosensors.

2. Results and Discussion

The Fe-N-C SACs were fabricated by pyrolysis of the mixture of metal salts, glucosamine, and silica templates.[6b] The transmission electron microscopy (TEM) image exhibits the hierarchically porous structure of the as-prepared Fe-N-C nanostructures (**Figure 1**A), and the average diameter of the abundant pores is ≈20 nm. The high-resolution TEM (HRTEM) image uncovers the curved graphene layers of Fe-N-C SACs (Figure 1B), and no metal nanoparticles are observed. Circled bright spots in the magnified high-resolution high-angle annular dark-field scanning transmission electron microscopy (HAADF-STEM) image (Z-contrast) correspond to single Fe atoms (Figure 1C). The selected area electron diffraction (SAED) pattern further confirms the inexistence of Fe nanoparticles and nanoclusters, as well as the disordered morphology of these stacked graphene layers (Figure 1D). Besides, the HAADF-STEM-energy dispersive spectroscopy (EDS) mapping images provide the elemental distribution of C, N, and Fe (Figure 1E–H). Then, X-ray diffraction (XRD) was employed to probe the graphitization degree of the Fe-N-C SAzymes (Figure S1, Supporting Information), two diffraction peaks can be assigned to carbon (002) and (101), respectively, and this result also supports that the Fe-N-C SACs do not contain Fe nanoparticles and nanoclusters, which agreed well with HRTEM image mentioned above. Raman spectra reveal that the addition of Fe species brings more defect sites to the Fe-N-C SACs (Figure S2, Supporting Information), these defects can be helpful for the catalytic process by improving the electron transfer between catalysts and substrates.[10,13] X-ray photoelectron spectroscopy (XPS) spectra demonstrate the existence of Fe-N coordination (Figure S3, Supporting Information). Meanwhile, X-ray absorption fine structure (XAFS) measurements were utilized to study the coordination environment of Fe atoms (Figure 1I,J), X-ray absorption near edge structure (XANES) spectra suggest that the valence state of Fe in the Fe-N-C SAzymes is between +2 and +3 in accordance with the chemical shift and the edge slope. Through the comparison of

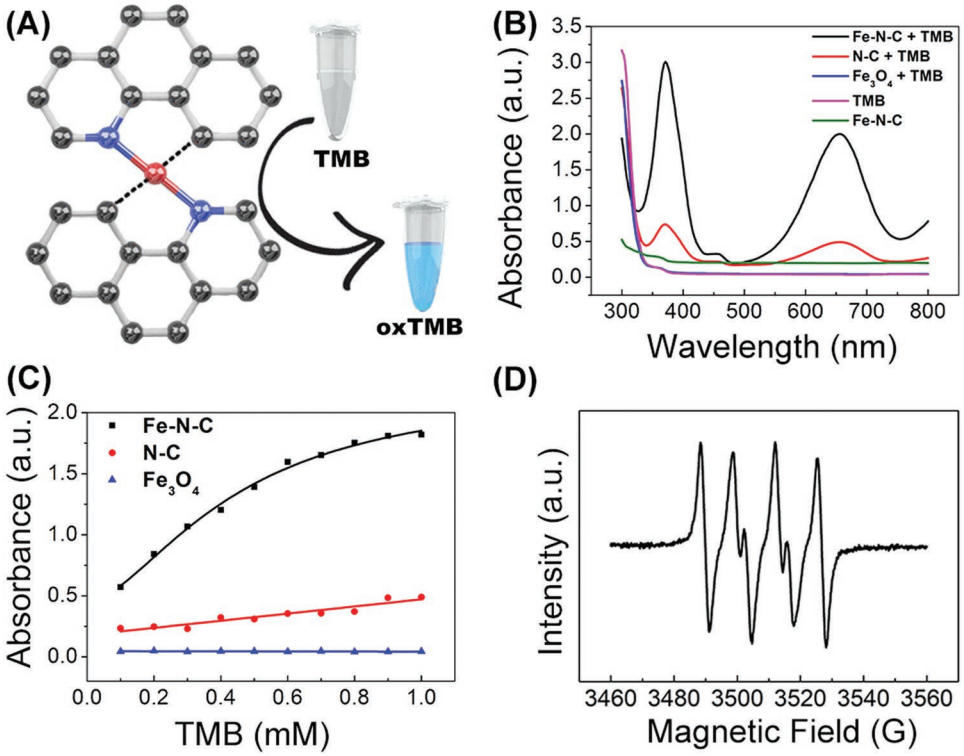

Figure 2. A) Schematic illustration of the oxidase-like activity of Fe-N-C SAzymes. B) UV–vis spectra of Fe-N-C SAzymes + TMB, N-C nanozymes + TMB, Fe_3O_4 + TMB, TMB, and Fe-N-C SAzymes in the acetate buffer. C) Comparison of the catalytic ability of Fe-N-C SAzymes, N-C nanozymes, and Fe_3O_4 in the acetate buffer after the addition of TMB from 0.1 to 1.0 × 10^{-3} M. D) EPR spectrum for detection of O_2^{-}• radicals.

the Fourier-transform extended X-ray absorption fine structure (EXAFS) spectrum of Fe-N-C SAzymes with those of Fe foils and iron phthalocyanine (FePc), Fe–N shell with a coordination number of ≈2.0 at a distance of 1.5 Å was suggested, indicating the presence of the atomically distribution of Fe.[6b]

Though various works have devoted to the study of peroxidase-like activity of Fe-based nanomaterials,[1a,14] few Fe-based nanomaterials with oxidase-like activity were reported.[15] To study the oxidase-like nanozyme property of Fe-N-C SAzymes, 3,3′,5,5′-tetramethylbenzidine (TMB) was employed as the allochroic substrates (**Figure 2**A). As shown in Figure 2B, Fe-N-C catalyzes the oxidation of TMB in the presence of O_2, and oxidation state of TMB (oxTMB) exhibit a blue color with a distinct absorption peak at 652 nm. The nanozyme performance of Fe-N-C follows the factors-dependent manner (e.g., concentration, reaction time, pH, and temperature) and these results were shown in Figure S4 (Supporting Information). Though N-C catalysts possess the intrinsic oxidase-like nanozyme property,[2a] Fe-N-C SAzymes owe superior oxidase-like activity in comparison to N-C (Figure 2C). Besides, Fe_3O_4 nanoparticles were also investigated for comparing the oxidase-like activity and no variation in absorbance was observed while the concentrations of TMB were increasing, which meant the lack of oxidase-like activity of Fe_3O_4 nanoparticles. Furthermore, the Michaelis–Menten constant (K_M) of Fe-N-C SAzymes was calculated as 1.81 × 10^{-3} M based on the kinetic assay (Figure S5, Supporting Information), which demonstrated the good affinity of Fe-N-C SAzymes toward TMB (Table S1, Supporting Information). To explore the role of O_2 in the reaction, two control experiments were carried out in O_2 and N_2-saturated solutions, respectively (Figure S6, Supporting Information). Notice that a distinct difference value was observed at 652 nm, verifying that O_2 takes part in this reaction to oxidize TMB. Then, dihydroethidine (DHE) were selected to study reactive radicals possibly involving O_2^{-}• (Figure S7, Supporting Information), an obvious peak at about 590 nm verified the presence of O_2^{-}•. Furthermore, electron paramagnetic resonance (EPR) spectrum supports the conclusion (Figure 2D). Based on the above results, the oxidase-like nanozyme activity of Fe-N-C can be capable of activating O_2 to generate O_2^{-}•, which further oxidize TMB.

As Lewis bases, thiols tend to coordinate with metal atoms. Based on this phenomenon, the mercapto molecules, cysteine (Cys) and glutathione (GSH), were used to study the influence on the activity of Fe-N-C SAzymes. As discussed above, single Fe atoms are believed to be the major active sites to mimic oxidase and Cys-blocked Fe-N-C SAzymes are expected to exhibit the lower nanozyme activity (**Figure 3**A). As expected, an obvious decrease in absorbance at 652 nm was observed once the addition of mercapto molecules (Figure 3B), which indicated the block of active sites of nanozymes. Fourier transform infrared spectroscopy (FTIR) was first used to ensure the attachment of the mercapto molecules (Figure 3C), the new peak at 3000–3200 cm^{-1} of Cys-treated Fe-N-C in contrast with Fe-N-C can be attributed to the stretching vibration of S—H bond of Cys. The disappearance of thiols peak may be caused by the coordination between Fe atoms and S atoms of thiols. XPS was employed for the further investigation of the electron density of S atoms to provide evidence of the coordination between Fe and thiols

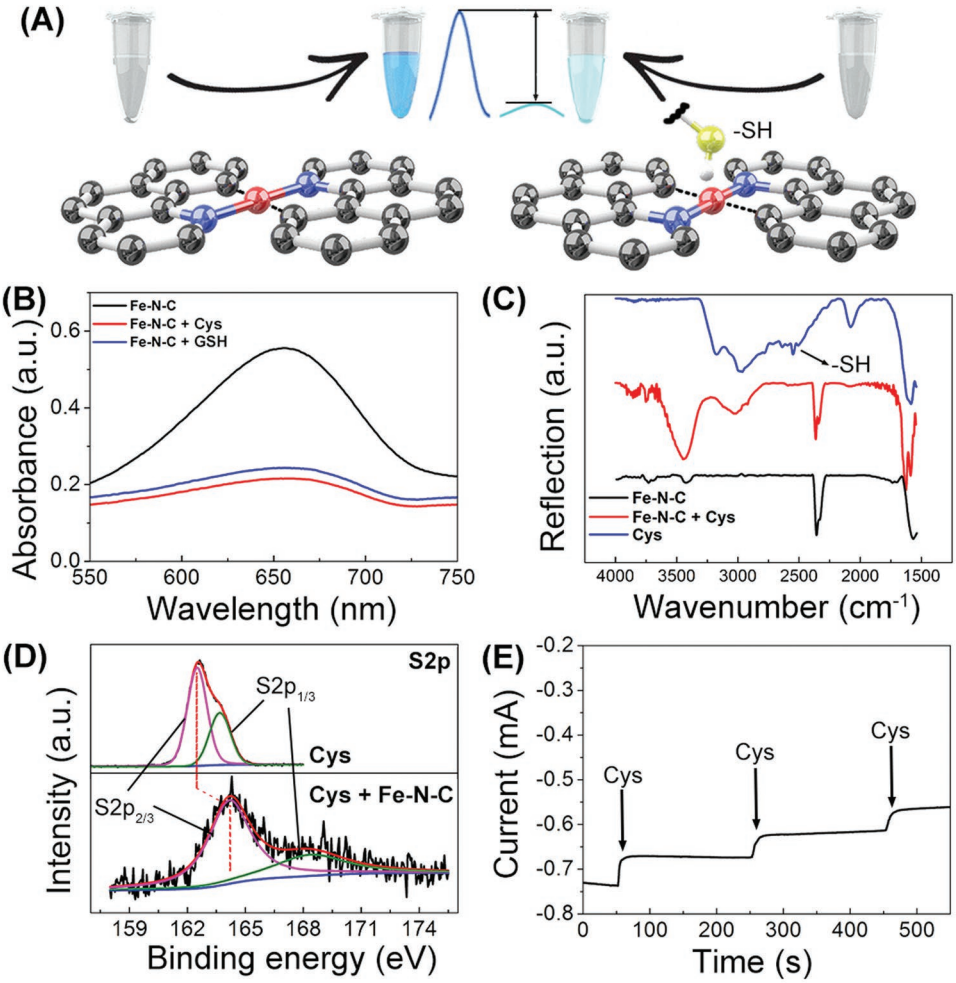

Figure 3. A) Schematic illustration of the inhibition of the oxidase-like activity of Fe-N-C SAzymes by mercapto molecules. B) UV–vis spectra of Fe-N-C SAzymes, and inhibited Fe-N-C by Cys and GSH, respectively, in the acetate buffer containing 0.2×10^{-3} M TMB. C) FTIR spectra of the Fe-N-C SAzymes, Cys-inhibited Fe-N-C, and Cys. D) S 2p XPS spectra for Cys and inhibited Fe-N-C by Cys. E) Current-time curve of Fe-N-C SACs in O_2-saturated acetate buffer with the addition of Cys.

(Figure 3D). Notably, the S 2p XPS peaks are shifted about 2.0 eV toward higher binding energy, which indicates the existence of strong coordination between Fe atoms and thiols.[16] Besides, the electrocatalytic behavior of inhibited Fe-N-C SAzymes for the oxygen reduction reaction was investigated (Figure 3E). Upon the addition of the Cys, the Fe-based active sites were poisoned, preventing the interaction with O_2 and thus weakening the electrocatalytic activity toward oxygen reduction.[17]

Mercapto molecules, like homocysteine, Cys and GSH, play critical roles in biological systems.[18] The levels of these mercapto biomolecules have a direct relationship between several diseases. Based on the inhibition mode, Fe-N-C SAzymes were successfully used to detect Cys and GSH (Figure S8, Supporting Information). For the potential application of SAzymes, Fe-N-C SAzymes were developed to evaluate the activity of AChE. AChE, as an enzyme of great importance in the nerve systems, acts as biomarkers in clinic diagnosis, drug screening, and environmental monitoring.[19] It is urgent to build robust biosensors for sensitive and convenient detection of AChE. AChE first catalyzes the hydrolysis of acetylthiocholine (ATCh) into thiocholine (TCh). Then, TCh, as one kind of mercapto molecules, blocks the active sites of Fe-N-C SAzymes and inhibits oxidase-like activity. As can be seen from **Figure 4**A, AChE can inhibit the activity of Fe-N-C SAzymes to some extent due to the profuse function groups of the enzyme, while Fe-N-C SAzymes in the enzyme-nanozyme system exhibit negligible activity upon the addition of ATCh. With the increasing amounts of AChE, Fe-N-C SAzymes retained less activity so that lower absorbance values were obtained (Figure 4B). Under the optimized conditions (Figure S9, Supporting Information), the relationship between calculated variations of absorbance and the activity of AChE was described in Figure 4C. Results showed that the Fe-N-C SAzymes-based biosensor can be used for the evaluation of AChE activity from 0.1 to 25 mU mL^{-1} with a limit of detection (LOD) of 0.014 mU mL^{-1}. With the comparison of former reports, the Fe-N-C SAzymes-TMB system exhibits a preferable performance (Table S2, Supporting Information). A series of proteins were used to examine the anti-interference ability of the biosensor (Figure 4D), and negligible changes were caused. Moreover, the recovery tests were

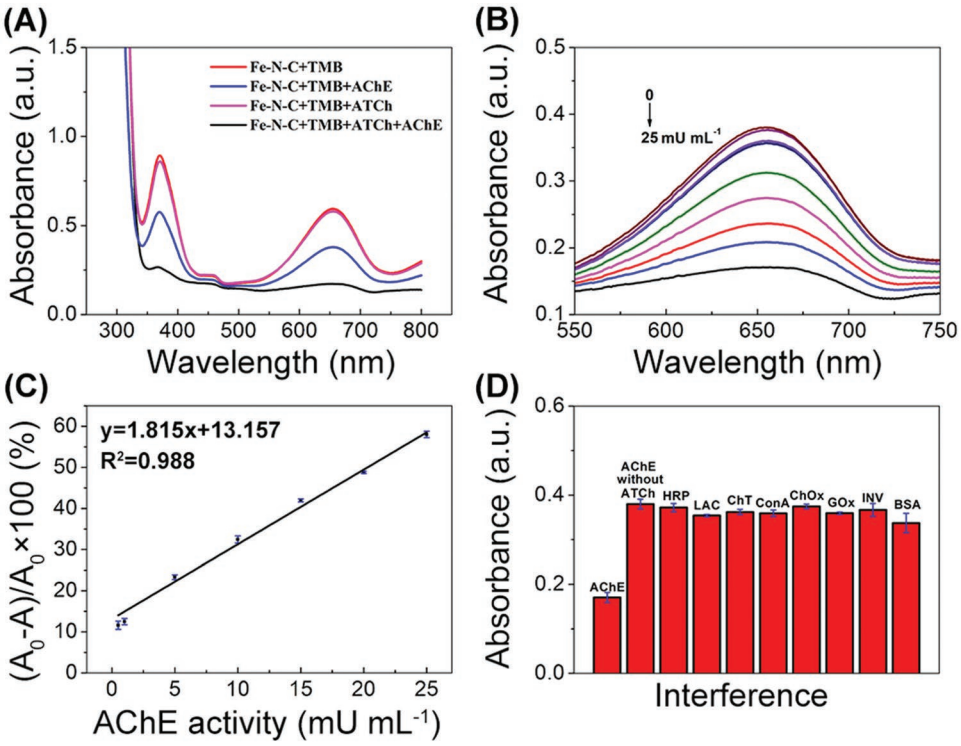

Figure 4. A) UV–vis spectra of AChE, ATCh, and AChE + ATCh in the acetate buffer containing Fe-N-C SAzymes and TMB. B) UV–vis spectra of the Fe-N-C SAzymes-TMB system in the presence of AChE from 0 to 25 mU mL^{-1}. C) The linear relationship between AChE activity and variations of absorbance values. D) Absorbance values at 652 nm of the Fe-N-C SAzymes-TMB system in the presence of different proteins as interference.

carried out to examine the practical feasibility. Two spiking levels of 10 and 20 mU mL^{-1} in the human serum were chosen, and the detection results were 9.5 and 18.9 mU mL^{-1}, with corresponding recovery rate of 95.0% and 94.6%, respectively.

Up to now, great efforts have been made to trace the amounts of OP,[20] which have wide usage in the agricultural area as pesticides but accompany with neurotoxicity toward human for inhibiting the activity of AChE.[21] Among them, the AChE-based biosensor is the main type biosensor to be employed for the detection of OP. Therefore, from a practical point of view, the AChE-Fe-N-C SAzymes-TMB system was employed for monitoring the amounts of OP. Paraoxon-ethyl was selected as the model of OP, which showed no effect on the activity of Fe-N-C SAzymes, and inhibited AChE (OP-AChE) exhibited the same inhibition effect as AChE toward Fe-N-C SAzymes (**Figure 5**A). The activity of AChE decreased with the addition of OP, so that the concentration of OP presented a positive correlation with the activity of Fe-N-C SAzymes. The calibration curve in Figure 5B shows that the biosensor could be used to detect OP within the concentrations range from 0.1 to 10 μg mL^{-1} with the LOD is 0.97 ng mL^{-1}. Also, a comparison with other nanozyme-based OP sensors in Table S3 (Supporting Information) demonstrates the good performance of the AChE-Fe-N-C SAzymes-TMB system.

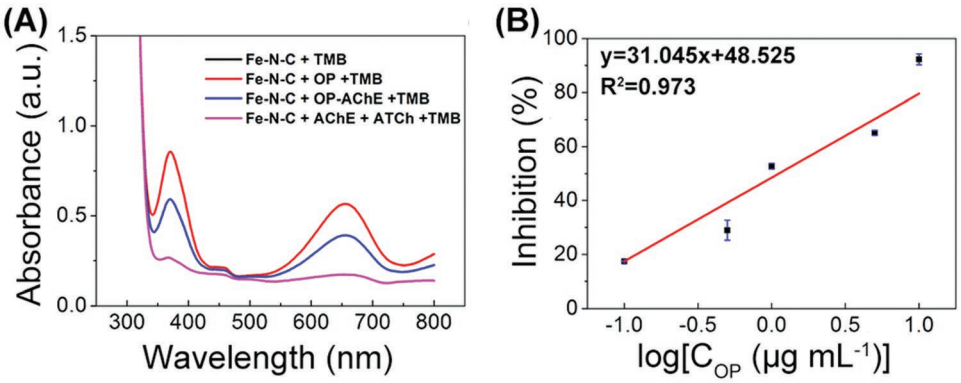

Figure 5. A) UV–vis spectra of Fe-N-C, Fe-N-C + OP, Fe-N-C + OP-AChE, and Fe-N-C + AChE + ATCh in the acetate buffer containing TMB. B) The linear relationship between the concentration of OP and inhibition rate.

3. Conclusion

In summary, the oxidase-like nanozyme activity of Fe-N-C SAzymes was investigated in this work. With the single Fe active sites, Fe-N-C SAzymes can activate O_2 into O_2^{-}• and trigger some oxidation reactions. Based on the fact that thiols inhibit the nanozyme activity, Fe-N-C SAzymes-TMB system was constructed for the evaluation of the AChE activity. Also, the AChE-Fe-N-C SAzymes-TMB biosensor was employed for tracing the amounts of OP. The successful demonstration of oxidase-like Fe-N-C SAzymes not only deepen the understanding of the nature of the biocatalysis but also provide practical applications in biosensors and other related fields.

4. Experimental Section

Materials: D-glucosamine hydrochloride, zinc chloride, iron (III) chloride hexahydrate, sodium acetate, and acetic acid were from sinopharm (Shanghai, China). Fe_3O_4 nanoparticles were purchased from Nachen Beijing. TMB, Cys, GSH, DHE, AChE (Electrophorus electricus Type VI-S, 245 units mg^{-1}), and ATCh chloride were from Sigma-Aldrich (St. Louis, MO). Paraoxon-ethyl was bought from Dr. Ehrenstorfer GmbH (Augsburg, Germany). All the chemical reagents obtained were of analytical reagent grade.

Instruments: TEM images were from Titan G260-300 (Thermo Fisher, USA). XAFS experiments on Fe K-edge were carried out in transmission mode at Beamline 20-BM-B of the APS. XPS measurements were performed by VG Multilab 2000 (Thermo Fisher, USA). XRD characterization was carried out by a D8 ADVANCE (Bruker, Germany). FTIR was characterized by a TENSOR27 (Bruker, USA). Raman spectra were measured using a Renishaw 1000 micro-Raman system. EPR spectra were obtained from Bruker A300. Electrochemical data were from a CHI 760E electrochemical workstation (Shanghai CH Instruments, China) at room temperature. All UV–vis spectra were from Cary 60 UV–vis (Agilent Technologies). All fluorescent spectra were from a multimode reader (Tecan Spark, Switzerland). A Milli-Q purification system (Millipore, MA) was used to obtain ultrapure water.

Synthesis of Fe-N-C SAzymes: For the synthesis of Fe-N-C SAzymes, 1.5 g SiO_2 suspension was used to dissolve the blend of 1.5 g glucosamine hydrochloride, $ZnCl_2$, and $FeCl_3$ (mole ratio 10:2:1). The solution was freeze-dried after stirring for 10 min. Then the powder was pyrolyzed under the nitrogen condition with a heating rate of 5 °C min^{-1} to 900 °C and kept for 2 h. At last, the Fe-N-C SAzymes were obtained through by hydrofluoric acid etching and then being freeze-dried. The synthesis of N-C nanozymes was similar to the strategy of Fe-N-C SAzymes except for the addition of $FeCl_3$.

Oxidase-Like Activity Experiments: Fe-N-C SAzymes, N-C nanozymes, and Fe_3O_4 nanoparticles were dispersed into water to a final concentration of 0.5 mg mL^{-1} and sonicated for 30 s before use. To compare the oxidase-like property and rule out the potential interference, 5 µL nanozyme solution was added into 0.4 mL 0.1 M acetate buffer (pH 4.0), 0.1 mL 1×10^{-3} M TMB was then added. After shaking under 37 °C for 15 min, the solution was analyzed to obtain the UV–vis spectra for the comparison of the nanozyme activity. And contrast experiments of TMB and Fe-N-C were carried out in the same situation without Fe-N-C and TMB, respectively.

For a further comparison of the nanozyme activity, a series concentration of TMB was prepared. Follow the above steps, the absorbance values at 652 nm were collected and the variation of them with the increasing concentration of TMB reflected the oxidase-like nanozyme activity.

Supporting Information

Supporting Information is available from the Wiley Online Library or from the author.

Acknowledgements

The authors gratefully acknowledge the financially supported by the Fundamental Research Funds for the Central Universities (CCNU19QN066), the Program of Introducing Talents of Discipline to Universities of China (111 program, B17019), and The Recruitment Program of Global Youth Experts of China.

Conflict of Interest

The authors declare no conflict of interest.

Keywords

acetylcholinesterase, biosensors, nanozymes, organophosphorus compounds, single-atom catalysts

Received: June 14, 2019
Revised: August 20, 2019
Published online:

[1] a) L. Gao, J. Zhuang, L. Nie, J. Zhang, Y. Zhang, N. Gu, T. Wang, J. Feng, D. Yang, S. Perrett, X. Yan, *Nat. Nanotechnol.* **2007**, *2*, 577; b) H. Wei, E. Wang, *Chem. Soc. Rev.* **2013**, *42*, 6060; c) J. Wu, X. Wang, Q. Wang, Z. Lou, S. Li, Y. Zhu, L. Qin, H. Wei, *Chem. Soc. Rev.* **2019**, *48*, 1004; d) Y. Huang, J. Ren, X. Qu, *Chem. Rev.* **2019**, *119*, 4357.

[2] a) K. Fan, J. Xi, L. Fan, P. Wang, C. Zhu, Y. Tang, X. Xu, M. Liang, B. Jiang, X. Yan, L. Gao, *Nat. Commun.* **2018**, *9*, 1440; b) Y. Zhao, Y. Huang, H. Zhu, Q. Zhu, Y. Xia, *J. Am. Chem. Soc.* **2016**, *138*, 16645; c) L. Han, H. Zhang, D. Chen, F. Li, *Adv. Funct. Mater.* **2018**, *28*, 1800018; d) Z. Wang, Y. Zhang, E. Ju, Z. Liu, F. Cao, Z. Chen, J. Ren, X. Qu, *Nat. Commun.* **2018**, *9*, 3334; e) N. Singh, G. Mugesh, *Angew. Chem., Int. Ed.* **2019**, *58*, 7797; f) H. Cheng, S. Lin, F. Muhammad, Y.-W. Lin, H. Wei, *ACS Sens.* **2016**, *1*, 1336.

[3] a) H. Zhang, G. Liu, L. Shi, J. Ye, *Adv. Energy Mater.* **2018**, *8*, 1701343; b) J. Liu, *ACS Catal.* **2017**, *7*, 34; c) Y. Chen, S. Ji, C. Chen, Q. Peng, D. Wang, Y. Li, *Joule* **2018**, *2*, 1242; d) C. Zhu, S. Fu, Q. Shi, D. Du, Y. Lin, *Angew. Chem., Int. Ed.* **2017**, *56*, 13944.

[4] a) B. Qiao, A. Wang, X. Yang, L. F. Allard, Z. Jiang, Y. Cui, J. Liu, J. Li, T. Zhang, *Nat. Chem.* **2011**, *3*, 634; b) X.-F. Yang, A. Wang, B. Qiao, J. Li, J. Liu, T. Zhang, *Acc. Chem. Res.* **2013**, *46*, 1740.

[5] a) J. Lin, A. Wang, B. Qiao, X. Liu, X. Yang, X. Wang, J. Liang, J. Li, J. Liu, T. Zhang, *J. Am. Chem. Soc.* **2013**, *135*, 15314; b) X. Li, W. Bi, L. Zhang, S. Tao, W. Chu, Q. Zhang, Y. Luo, C. Wu, Y. Xie, *Adv. Mater.* **2016**, *28*, 2427; c) G. Vilé, D. Albani, M. Nachtegaal, Z. Chen, D. Dontsova, M. Antonietti, N. López, J. Pérez-Ramírez, *Angew. Chem., Int. Ed.* **2015**, *54*, 11265; d) G. Gao, Y. Jiao, E. R. Waclawik, A. Du, *J. Am. Chem. Soc.* **2016**, *138*, 6292; e) G. Liu, A. W. Robertson, M. M.-J. Li, W. C. H. Kuo, M. T. Darby, M. H. Muhieddine, Y.-C. Lin, K. Suenaga, M. Stamatakis, J. H. Warner, S. C. E. Tsang, *Nat. Chem.* **2017**, *9*, 810; f) C. Zhu, Q. Shi, S. Feng, D. Du, Y. Lin, *ACS Energy Lett.* **2018**, *3*, 1713.

[6] a) C. Zhu, S. Fu, J. Song, Q. Shi, D. Su, M. H. Engelhard, X. Li, D. Xiao, D. Li, L. Estevez, D. Du, Y. Lin, *Small* **2017**, *13*, 1603407; b) C. Zhu, Q. Shi, B. Z. Xu, S. Fu, G. Wan, C. Yang, S. Yao, J. Song, H. Zhou, D. Du, S. P. Beckman, D. Su, Y. Lin, *Adv. Energy Mater.* **2018**, *8*, 1801956; c) S. Fu, C. Zhu, D. Su, J. Song, S. Yao, S. Feng, M. H. Engelhard, D. Du, Y. Lin, *Small* **2018**, *14*, 1703118; d) J. Li, M. Chen, D. A. Cullen, S. Hwang, M. Wang, B. Li, K. Liu, S. Karakalos, M. Lucero, H. Zhang, C. Lei, H. Xu, G. E. Sterbinsky, Z. Feng, D. Su, K. L. More, G. Wang, Z. Wang, G. Wu, *Nat. Catal.* **2018**, *1*, 935; e) H. Shen, E. Gracia-Espino, J. Ma, H. Tang, X. Mamat, T. Wagberg, G. Hu, S. Guo, *Nano Energy* **2017**, *35*, 9.

[7] a) A. B. McQuarters, M. W. Wolf, A. P. Hunt, N. Lehnert, *Angew. Chem., Int. Ed.* **2014**, *53*, 4750; b) X. Huang, J. T. Groves, *Chem. Rev.* **2018**, *118*, 2491.

[8] a) C. Zhao, C. Xiong, X. Liu, M. Qiao, Z. Li, T. Yuan, J. Wang, Y. Qu, X. Wang, F. Zhou, Q. Xu, S. Wang, M. Chen, W. Wang, Y. Li, T. Yao, Y. Wu, Y. Li, *Chem. Commun.* **2019**, *55*, 2285; b) W. Ma, J. Mao, X. Yang, C. Pan, W. Chen, M. Wang, P. Yu, L. Mao, Y. Li, *Chem. Commun.* **2019**, *55*, 159; c) L. Jiao, H. Yan, Y. Wu, W. Gu, C. Zhu, D. Du, Y. Lin, *Angew. Chem., Int. Ed.* **2019**, https://doi.org/10.1002/anie.201905645; d) N. Cheng, J.-C. Li, D. Liu, Y. Lin, D. Du, *Small* **2019**, https://doi.org/10.1002/smll.201901485; e) L. Huang, J. Chen, L. Gan, J. Wang, S. Dong, *Sci. Adv.* **2019**, *5*, eaav5490.

[9] M. Huo, L. Wang, Y. Wang, Y. Chen, J. Shi, *ACS Nano* **2019**, *13*, 2643.

[10] B. Xu, H. Wang, W. Wang, L. Gao, S. Li, X. Pan, H. Wang, H. Yang, X. Meng, Q. Wu, L. Zheng, S. Chen, X. Shi, K. Fan, X. Yan, H. Liu, *Angew. Chem., Int. Ed.* **2019**, *58*, 4911.

[11] X. Li, X. Huang, S. Xi, S. Miao, J. Ding, W. Cai, S. Liu, X. Yang, H. Yang, J. Gao, J. Wang, Y. Huang, T. Zhang, B. Liu, *J. Am. Chem. Soc.* **2018**, *140*, 12469.

[12] a) B. Liu, Z. Sun, P.-J. J. Huang, J. Liu, *J. Am. Chem. Soc.* **2015**, *137*, 1290; b) P. Weerathunge, R. Ramanathan, V. A. Torok, K. Hodgson, Y. Xu, R. Goodacre, B. K. Behera, V. Bansal, *Anal. Chem.* **2019**, *91*, 3270; c) P. Zhang, D. Sun, A. Cho, S. Weon, S. Lee, J. Lee, J. W. Han, D.-P. Kim, W. Choi, *Nat. Commun.* **2019**, *10*, 940.

[13] G. Zhang, M. Zhang, X. Ye, X. Qiu, S. Lin, X. Wang, *Adv. Mater.* **2014**, *26*, 805.

[14] Z. Zhang, X. Zhang, B. Liu, J. Liu, *J. Am. Chem. Soc.* **2017**, *139*, 5412.

[15] a) H. Zhang, J. Chen, Y. Yang, L. Wang, Z. Li, H. Qiu, *Anal. Chem.* **2019**, *91*, 5004; b) Q. Chen, C. Liang, X. Zhang, Y. Huang, *Talanta* **2018**, *182*, 476.

[16] X. Cui, J. Wang, B. Liu, S. Ling, R. Long, Y. Xiong, *J. Am. Chem. Soc.* **2018**, *140*, 16514.

[17] J. Masa, W. Xia, M. Muhler, W. Schuhmann, *Angew. Chem., Int. Ed.* **2015**, *54*, 10102.

[18] X. Chen, Y. Zhou, X. Peng, J. Yoon, *Chem. Soc. Rev.* **2010**, *39*, 2120.

[19] H. Soreq, S. Seidman, *Nat. Rev. Neurosci.* **2001**, *2*, 294.

[20] a) Y. Wu, L. Jiao, W. Xu, W. Gu, C. Zhu, D. Du, Y. Lin, *Small* **2019**, *15*, 1900632; b) Y. Zhao, M. Yang, Q. Fu, H. Ouyang, W. Wen, Y. Song, C. Zhu, Y. Lin, D. Du, *Anal. Chem.* **2018**, *90*, 7391.

[21] Y. Miao, N. He, J.-J. Zhu, *Chem. Rev.* **2010**, *110*, 5216.